

# Critical exponent of metal-insulator transition in doped semiconductors using density functional theory and local density approximation

Yosuke Harashima\* and Keith Slevin

*Department of Physics, Graduate School of Science, Osaka University,  
1-1 Machikaneyama, Toyonaka, Osaka 560-0043, Japan*

(Dated: December 3, 2024)

We report a simulation of the metal-insulator transition in a model of a doped semiconductor that treats disorder and interactions on an equal footing. The model is analysed using density functional theory. From a multi-fractal analysis of the Kohn-Sham eigenfunctions, we find  $\nu \approx 1.3$  for the critical exponent of the correlation length. This differs from that of Anderson's model of localisation and suggests that the Coulomb interaction changes the universality class of the transition.

In heavily doped semiconductors a zero temperature metal-insulator transition (MIT) is observed as a function of doping concentration  $N_d$ . For samples with doping concentrations below a critical concentration  $N_c$ , the conductivity extrapolated to zero temperature  $\sigma(T=0)$  is found to be zero, while for samples with concentrations exceeding this critical concentration,  $\sigma(T=0)$  is finite. Well studied examples are the transition in Si:P [1–3] and Ge:Ga [4] and there are many others (see [4] and references therein). The observed critical concentrations obey, approximately at least, the relation[5]

$$N_c^{\frac{1}{3}} a_B^* \approx 0.26. \quad (1)$$

Here,  $a_B^* \equiv (\epsilon_r/m^*)a_B$  is the effective Bohr radius of a hydrogenic impurity state for a carrier with effective mass  $m^*$  in a medium with relative dielectric constant  $\epsilon_r$ .

The transition is continuous and considerable effort has been expended to study the critical phenomena observed at the transition and the associated critical exponents, the values of which are expected to be universal. As the transition is approached from higher concentration  $N_d > N_c$  it is found that the zero temperature conductivity obeys a power law with a critical exponent  $\mu$

$$\sigma(N_d, T=0) \propto (N_d - N_c)^\mu. \quad (2)$$

Analyses have also been performed which avoid the extrapolation to zero temperature and fit data at finite temperatures directly to the dynamic scaling law[6]

$$\sigma(N_d, T) = T^x f((N_d/N_c - 1)T^{-y}) \quad (3)$$

Here,  $x = 1/z$  and  $y = 1/(z\nu)$  with  $\nu$  the critical exponent describing the divergence of the correlation length at the transition and  $z$  the dynamic exponent. Demanding consistency between these scaling laws gives  $\mu = \nu$ , which is known as Wegner's scaling relation.

For Si:P there has been debate over the value of the critical exponent;  $\mu \approx 0.5$  or  $\mu \approx 1.3$ [7, 8]. Itoh et al addressed this controversy by a careful study of the MIT in

neutron transmutation doped Ge:Ga [4]. They demonstrated that the width of the critical region depends on the compensation. For intentionally compensated samples they found both Eq. (2) and dynamic scaling Eq. (3) are observed with  $\mu \approx 1$  and  $z \approx 3$ . In nominally uncompensated samples, Eq. (2) with  $\mu \approx 0.5$  is observed over a wide range of concentrations on the metallic side but dynamic scaling is violated. However, when attention is focused on a much narrower region around the critical point, Eq. (2) with  $\mu \approx 1$  is a better fit and dynamic scaling is recovered with  $\mu \approx 1$  and  $z \approx 3$ . Dynamic scaling with similar values of the exponents has also been reported in Si:P[3].

There is still no explanation of the critical behaviour described above. Since the impurities used to dope the semiconductor are randomly distributed in space, an Anderson transition is a possibility. However, the value of the critical exponent is not consistent with this. While  $z = 3$  is expected for Anderson's model of localisation since the only relevant energy scale at the transition is the level spacing, numerical finite size scaling studies[9–11] of this model have established unambiguously that  $\nu \approx 1.6$  to within a precision of a few percent. Clear demonstrations of the universality of this value include its confirmation in a non-interacting tight-binding model with random hopping of a doped semiconductor[12], and its experimental measurement in a quasi-periodic atomic kicked rotor[13]. This suggests that an explanation of the critical behaviour must incorporate both electron-electron interactions and disorder. While there have been serious efforts to develop such a theory (see [14, 15] for an up to date discussion), it remains one of the most challenging problems in condensed matter physics.

The object of this paper is to take a step closer to an understanding of the MIT in doped semiconductors by determining how the Coulomb interaction affects the critical behaviour of the Anderson transition. We do this by simulating a model of a doped semiconductor that treats on an equal footing both the disorder due to the random spatial distribution of the dopants and the Coulomb interaction between the carriers. Applying a multi-fractal

analysis, we find that the model exhibits a localization-delocalization transition at approximately the right carrier concentration (see Figure 1). Moreover, we find that the critical exponent  $\nu \approx 1.3$ , which is different from that for the standard Anderson transition.

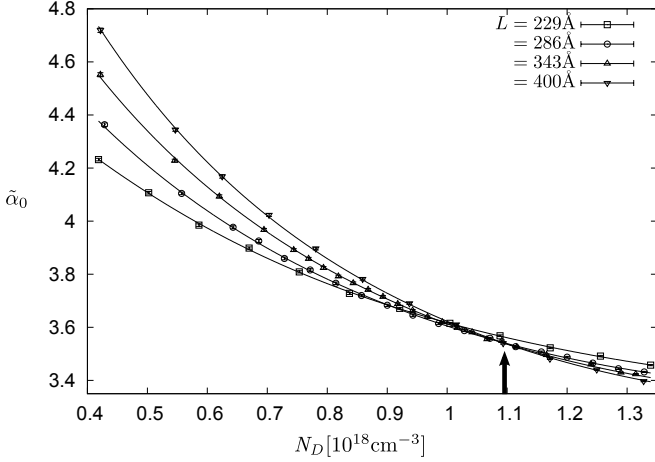


FIG. 1. The generalized multi-fractal exponent  $\tilde{\alpha}_0$  as a function of donor concentration for several system sizes. The solid lines are a finite size scaling fit to the data. The critical concentration is indicated by an arrow.

The main difficulty in a numerical study of this problem is to find a model that is numerically tractable but still captures the physics of both disorder and interactions. The wide applicability of the Mott criterion suggests that a good starting point is to treat the semiconductor as an effective medium with appropriate dielectric constant and effective mass. The donors are modelled as unit positive charges randomly distributed in this medium. The Hamiltonian (in Hartree atomic units) is [16]

$$\mathcal{H} = -\frac{1}{2m^*} \sum_{i=1}^N \nabla_i^2 - \frac{1}{\epsilon_r} \sum_{i,I=1}^N \frac{1}{|\mathbf{r}_i - \mathbf{R}_I|} + \frac{1}{2\epsilon_r} \sum_{i \neq j}^N \frac{1}{|\mathbf{r}_i - \mathbf{r}_j|} + \frac{1}{2\epsilon_r} \sum_{I \neq J}^N \frac{1}{|\mathbf{R}_I - \mathbf{R}_J|} \quad (4)$$

Here,  $\{\mathbf{R}_I\}$  are the random positions of the donors and  $N$  is the number of donors. Each impurity donates a single electron so the number of electrons is also  $N$  and the total charge is zero.

Below, for ease of comparison with experiment we use the values for silicon  $m^* = 0.32$  and  $\epsilon_r = 12$ . However, we emphasise that the properties of this model scale exactly with the dielectric constant and effective mass. Thus, for example, the Mott criterion must be obeyed, though with a constant on the right hand side that will be determined numerically below.

The next question is how to treat the model. To study a phase transition we need to consider a reasonably large

number of electrons, so exact diagonalization is impractical. Instead we use the Kohn-Sham (KS) formulation of density functional theory (DFT) [17, 18]. The KS eigenfunctions  $\psi_i$  and eigenvalues  $\epsilon_i$  satisfy

$$\left( -\frac{1}{2m^*} \nabla^2 + V_{\text{eff}} \right) \psi_i(\mathbf{r}) = \epsilon_i \psi_i(\mathbf{r}) \quad (5)$$

The effective potential

$$V_{\text{eff}} = V_{\text{ext}} + V_{\text{Hartree}} + V_{\text{XC}} \quad (6)$$

appearing in these equations is comprised of three terms. The first is the random potential due to the donors

$$V_{\text{ext}}(\mathbf{r}) = -\frac{1}{\epsilon_r} \sum_{I=1}^N \frac{1}{|\mathbf{r} - \mathbf{R}_I|} \quad (7)$$

The second is the Hartree potential

$$V_{\text{Hartree}}(\mathbf{r}) = \frac{1}{\epsilon_r} \int d^3r' \frac{n(\mathbf{r}')}{|\mathbf{r} - \mathbf{r}'|} \quad (8)$$

where

$$n(\mathbf{r}) = \sum_{i=1}^N |\psi_i(\mathbf{r})|^2 \quad (9)$$

is the number density of electrons. The third is the exchange-correlation potential which is given by the functional derivative of the exchange-correlation energy functional  $E_{\text{XC}}[n]$  with respect to the number density

$$V_{\text{XC}}(\mathbf{r}) = \frac{\delta E_{\text{XC}}}{\delta n(\mathbf{r})}. \quad (10)$$

If this functional were known exactly, the solution of the KS equations would yield the exact ground state density and energy of the interacting system. In practice, the exact form of the exchange-correlation energy functional is not known and an approximation is required. In this work, we use the local density approximation (LDA)

$$E_{\text{XC}} \approx E_{\text{XC}}^{\text{LDA}} \equiv \int d^3r \epsilon_{\text{XC}}(n(\mathbf{r})) n(\mathbf{r}). \quad (11)$$

To render the model more numerically tractable we also assume complete spin polarization. (This is an important approximation and will be discussed further below.) For  $\epsilon_{\text{XC}}$  we use the form given in Eq. (2) of [19], where we set spin polarization  $\zeta = 1$  and we use the parameter values of [20]. Note that the expression given in these references are for free space. To use them for our effective medium we need to rescale lengths and energies according to  $\tilde{\mathbf{r}} = (m^*/\epsilon_r) \mathbf{r}$  and  $\tilde{E} = (\epsilon_r^2/m^*) E$ , respectively, where the tilde indicates the free space quantity.

For numerical purpose we replace the continuous effective medium with an  $L \times L \times L$  cubic grid. Eq. (5) is replaced with a next-nearest neighbour finite difference approximation. In the LDA the resulting matrix equations

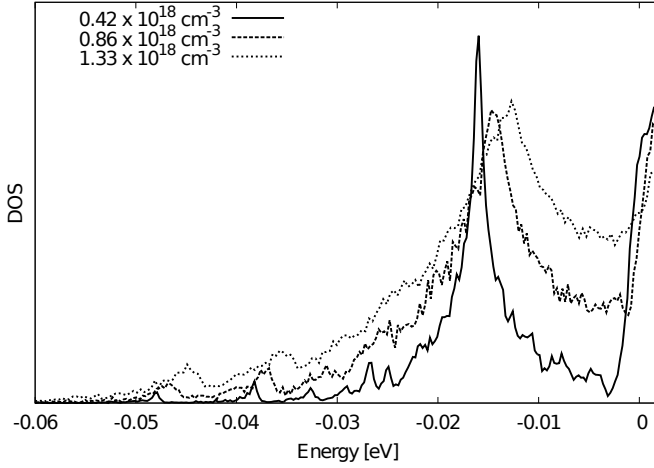


FIG. 2. The average density of states for a random spatial distribution of donor impurities.

are sparse and the eigenvectors and eigenvalues of the occupied states can be found using iterative techniques[21]. The potential due to the impurities and the Hartree potential are found using fast Fourier transform. The self-consistent solution of the equations is found iteratively starting from an initial guess for the KS eigenfunctions. For details the reader is referred to [16].

As we describe below, we observe a localisation-delocalisation transition of the highest occupied KS eigenfunctions as a function of donor concentration. We have analysed this using a multi-fractal finite size scaling method[10, 11] that has been successfully applied to the Anderson transition. Before describing this, however, we report results for the density of states (DOS), or more strictly speaking, the density of KS eigenvalues.

For the unphysical situation that the donors are regularly arranged on a simple cubic lattice, we have found that the impurity band merges with the conduction band at  $N_d \approx 1.59 \times 10^{18} \text{cm}^{-3}$ . The average DOS for the more realistic random distribution of donors is shown, for several concentrations, in Fig. 2. In this case, the bands merge at a much smaller concentration of  $N_d \approx 0.4 \times 10^{18} \text{cm}^{-3}$ . We should note this value is not directly comparable with experiment for two reasons. First, we have assumed complete spin polarization. Second, the LDA is known to underestimate band gaps. Nevertheless, we can be sure that the MIT we observe below occurs after the impurity and conduction bands have merged.

We now turn to the multi-fractal analysis. We divide the  $L \times L \times L$  system into boxes of linear size  $l$ . We define a coarse grained intensity  $\{\mu_k\}$  by

$$\mu_k \equiv \int_k d^3r |\psi(\mathbf{r})|^2. \quad (12)$$

The subscript,  $k$ , indexes the  $(N/l)^3$  boxes. To analyze the transition we focus on the intensity distribution of

the highest occupied KS orbital. We define a generalized inverse participation ratio by

$$R_q \equiv \sum_k (\mu_k)^q \quad (13)$$

and the related quantity obtained by its differentiation with respect to the exponent  $q$

$$S_q \equiv \sum_k (\mu_k)^q \ln \mu_k \quad (14)$$

Generalized multi-fractal exponents  $\tilde{\tau}_q$  and  $\tilde{\alpha}_q$  are defined from these

$$\tilde{\tau}_q \equiv \frac{\ln \langle R_q \rangle}{\ln \lambda} \quad (15)$$

$$\tilde{\alpha}_q \equiv \frac{\langle S_q \rangle}{\langle R_q \rangle \ln \lambda} \quad (16)$$

Here,  $\lambda$  is the ratio of box size to system size

$$\lambda \equiv \frac{l}{L} \quad (17)$$

In the limit  $\lambda \rightarrow 0$  the generalised exponents become the standard multi-fractal exponents.

We proceed by assuming that, in the vicinity of the critical donor concentration, the generalised multi-fractal exponents obey the scaling law[11]

$$\Gamma(N_d, L, l) = F(\phi_1 L^{1/\nu}, \phi_2 L^{y_2}, \lambda) \quad (18)$$

Here,  $\Gamma$  indicates  $\tilde{\tau}_q$  or  $\tilde{\alpha}_q$ ,  $\phi_1$  is a relevant scaling variable, and  $\phi_2$  an irrelevant scaling variable with irrelevant exponent  $y_2 < 0$ . (For brevity, the dependence on  $q$  is not written explicitly.) The scaling variables are functions of the reduced impurity donor concentration

$$n_r \equiv \frac{N_d - N_c}{N_c} \quad (19)$$

To apply standard finite size scaling we fix  $\lambda$  at a constant value, i.e. we scale the box size simultaneously with the system size so that we can omit the dependence on  $\lambda$

$$\Gamma(N_d, L) = F(\phi_1 L^{1/\nu}, \phi_2 L^{y_2}) \quad (20)$$

The correlation length,  $\xi$ , is given by

$$\xi = \xi_0 |\phi_1(n_r)|^{-\nu} \quad (21)$$

with  $\xi_0$  a constant. We allow for non-linearity of  $\phi_1$  and  $\phi_2$  by expanding them as

$$\phi_1(n_r) = \sum_{i=1}^{m_1} a_i n_r^i \quad \phi_2(n_r) = \sum_{i=0}^{m_2} b_i n_r^i \quad (22)$$

At the critical point  $\phi_1$  must be zero, so we fix the constant term in the expansion to zero. The scaling function Eq. (20) is expanded as

$$F(X, Y) = \sum_{i,j=0}^{n_1, n_2} F_{ij} X^i Y^j. \quad (23)$$

We estimate the critical concentration and the critical exponent by fitting this model to our simulation data.

Simulations were performed for systems sizes in the range  $L = 229 \sim 400\text{\AA}$  and donor concentrations of  $N_d \equiv N/L^3 = 0.4 \sim 1.3 \times 10^{18}\text{cm}^{-3}$ . This corresponds to a number of electrons of  $5 \sim 85$ . We set the finite difference grid spacing to 18 Bohr, which is about half of the effective Bohr radius for Si. The donors were randomly distributed on a simple cubic lattice with spacing 36 Bohr. This avoids the situation that two donors are unphysically close. The number of samples for each system size and donor concentration varies between 1500 and 3000. For a few percent of samples, the self-consistent calculation does not converge. These samples are neglected in the analysis. For the multi-fractal analysis we set  $\lambda = 1/6$ .

Fig. 1 shows the generalised exponent  $\tilde{\alpha}_0$  as a function of the donor concentration. For low concentration  $\tilde{\alpha}_0$  increases with system size. This is the typical behavior for localized states. Opposite behavior, typical of extended states, is found for higher concentration. The scale invariant point between these concentration regions indicates the transition. The solid lines in Fig. 1 are the result of fitting the finite size scaling model to the data. The number of data points is 67. The orders of the expansions are  $m_1 = 2$ ,  $m_2 = 1$ ,  $n_1 = 3$ ,  $n_2 = 1$  and the number of corresponding fitting parameters is 13. The critical concentration and critical exponent obtained from the fitting are  $N_c = 1.09(+0.07, -0.01) \times 10^{18}\text{cm}^{-3}$  and  $\nu = 1.30(+0.12, -0.06)$ . The errors are 95% confidence intervals obtained by Monte Carlo simulation.

The estimates of the critical concentration and the critical exponent should not depend on  $q$ . To check this, we performed the multi-fractal analysis for various  $q = -0.75 \sim 1.25$ . The results are shown in Fig. 3. On the one hand, the estimate of the critical concentration varies by about 20% for the range of  $q$  considered, which is not completely satisfactory. On the other hand, the estimate of the critical exponent is independent of  $q$ .

The measured critical concentration for Si:P is  $3.52 \times 10^{18}\text{cm}^{-3}$ . The predicted critical concentration based on the Mott criterion is  $2.25 \times 10^{18}\text{cm}^{-3}$  and we should certainly not expect to do better than this in a theoretical approach that uses an effective medium. The MIT in our model occurs at  $1 \sim 1.2 \times 10^{18}\text{cm}^{-3}$  which corresponds to a value of 0.2 in the Mott criterion. Possible explanations for this discrepancy include the neglect of the spin degree of freedom and limitations of the LDA.

Our result for the critical exponent,  $\nu \approx 1.30$ , should have a wide applicability since the values of critical exponents are universal. While our range of system sizes is limited, the  $q$  independence of the estimate of the exponent seen in Fig. 3 gives us some confidence that the critical exponent is different from that of the standard Anderson model. This is at first sight puzzling because the KS equations are in the same Dyson symmetry class

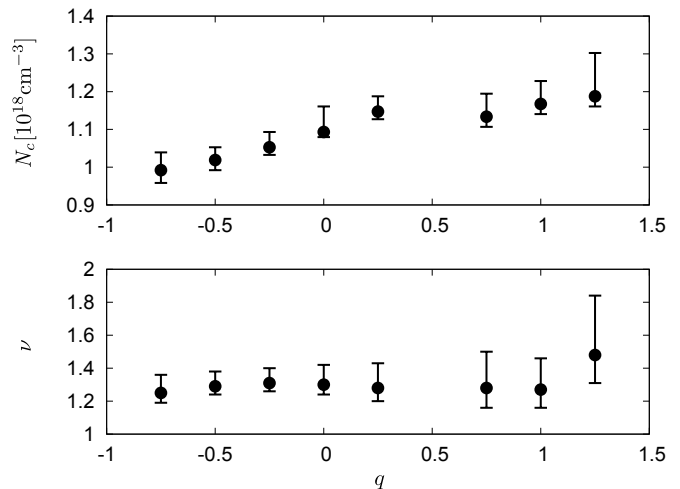


FIG. 3. The estimates of the critical concentration  $N_c$  and the critical exponent  $\nu$  obtained for different powers  $q$ . The data shown above is estimated from  $\alpha_q$  and similar behaviour can be observed for  $\tau_q$ .

as Anderson's model of localisation. A possible explanation of the different value for the exponent are the spatial correlations in the effective potential  $V_{\text{eff}}$ .

This study could be extended in several ways. It should be possible to study the role of compensation by introducing negatively charged donors. The restriction of complete spin polarization may be relaxed by using the local spin density approximation. This is particularly important since local moments play an important role [14, 22–26]. Also, while DFT gives the density of the true many body ground state, the Slater determinant of the KS eigenfunctions is only an approximation to its wavefunction. The current calculation may be a starting point for many-body perturbation calculations such as the *GW* approximation.

We thank Stefan Kettemann and Tomi Ohtsuki for critical readings of this manuscript, and the Advanced Materials Science division of POSTECH for its hospitality during visits in the course of this work. Part of the computations were performed using the Supercomputer Center, ISSP, the University of Tokyo. This work was supported by Global COE Program (Core Research and Engineering of Advanced Materials-Interdisciplinary Education Center for Materials Science), MEXT, Japan.

\* Present address: Elements Strategy Initiative Center for Magnetic Materials, National Institute for Materials Science, 1-2-1 Sengen, Tsukuba, Ibaraki 305-0047, Japan

- [1] T. F. Rosenbaum, K. Andres, G. A. Thomas, and R. N. Bhatt, Phys. Rev. Lett. **45**, 1723 (1980).
- [2] H. Stupp, M. Hornung, M. Lakner, O. Madel, and H. v.

- Lohneysen, Phys. Rev. Lett. **71**, 2634 (1993).
- [3] H. Löhneysen, Annalen der Physik **523**, 599 (2011).
  - [4] K. M. Itoh, M. Watanabe, Y. Ootuka, E. E. Haller, and T. Ohtsuki, JPSJ **73**, 173 (2004).
  - [5] P. P. Edwards and M. J. Sienko, Phys. Rev. B **17**, 2575 (1978).
  - [6] F. J. Wegner, Zeitschrift für Physik B Condensed Matter **25**, 327 (1976).
  - [7] T. F. Rosenbaum, G. A. Thomas, and M. A. Paalanen, Phys. Rev. Lett. **72**, 2121 (1994).
  - [8] H. Stupp, M. Hornung, M. Lakner, O. Madel, and H. v. Lohneysen, Phys. Rev. Lett. **72**, 2122 (1994).
  - [9] K. Slevin and T. Ohtsuki, Phys. Rev. Lett. **82**, 382 (1999).
  - [10] A. Rodriguez, L. J. Vasquez, K. Slevin, and R. A. Römer, Phys. Rev. Lett. **105**, 046403 (2010).
  - [11] A. Rodriguez, L. J. Vasquez, K. Slevin, and R. A. Römer, Phys. Rev. B **84**, 134209 (2011).
  - [12] J. J. Krich and A. Aspuru-Guzik, Phys. Rev. Lett. **106**, 156405 (2011).
  - [13] M. Lopez, J.-F. Clément, P. Szriftgiser, J. C. Garreau, and D. Delande, Phys. Rev. Lett. **108**, 095701 (2012).
  - [14] A. M. Finkel'stein, International Journal of Modern Physics B **24**, 1855 (2010).
  - [15] V. Dobrosavljevic, N. Trivedi, and J. M. Valles, *Conductor-insulator quantum phase transitions* (Oxford University Press, Oxford, 2012).
  - [16] Y. HARASHIMA and K. SLEVIN, International Journal of Modern Physics Conference Series (IJMPCS) **11**, 90 (2012).
  - [17] P. Hohenberg and W. Kohn, Phys. Rev. **136**, B864 (1964).
  - [18] W. Kohn and L. J. Sham, Phys. Rev. **140**, A1133 (1965).
  - [19] O. Gunnarsson, B. I. Lundqvist, and J. W. Wilkins, Phys. Rev. B **10**, 1319 (1974).
  - [20] J. F. Janak, V. L. Moruzzi, and A. R. Williams, Phys. Rev. B **12**, 1257 (1975).
  - [21] M. Bollhfer and Y. Notay, Computer Physics Communications **177**, 951 (2007).
  - [22] R. N. Bhatt and D. S. Fisher, Phys. Rev. Lett. **68**, 3072 (1992).
  - [23] D. Belitz and T. R. Kirkpatrick, Rev. Mod. Phys. **66**, 261 (1994).
  - [24] S. Kettemann, E. R. Mucciolo, and I. Varga, Phys. Rev. Lett. **103**, 126401 (2009).
  - [25] S. Kettemann, E. R. Mucciolo, I. Varga, and K. Slevin, Phys. Rev. B **85**, 115112 (2012).
  - [26] A. C. Potter, M. Barkeshli, J. McGreevy, and T. Senthil, Phys. Rev. Lett. **109**, 077205 (2012).